Eur. Phys. J. A **21**, 273–279 (2004)
DOI 10.1140/epja/i2003-10215-y

THE EUROPEAN PHYSICAL JOURNAL A

A study of proton-induced reactions at 190 MeV

B. Mukherjee[1,a], J.C.S. Bacelar[1], J.P.M. Beijers[1], M.N. Harakeh[1], N. Kalantar-Nayestanaki[1], M. Kiš[1], H. Löhner[1], M. Mahjour-Shafiei[1], and P. Henrotte[2]

[1] Kernfysisch Versneller Instituut (KVI), Zernikelaan 25, 9747 AA Groningen, The Netherlands
[2] Institut de Physique, Université de Liège, Belgium

Received: 11 November 2003 / Revised version: 9 February 2004 /
Published online: 31 August 2004 – © Società Italiana di Fisica / Springer-Verlag 2004
Communicated by M. Garçon

Abstract. Differential cross-sections and proton multiplicities, resulting from the bombardment of ^{56}Fe, ^{208}Pb, and ^{238}U targets by a 190 MeV proton beam were measured for the first time. Data were taken over two different angular ranges 5°–30° and 91°–160° with two different detection systems. Angular distributions of fast (> 20 MeV) protons are all forward peaked, due to the dominating elastic-scattering contribution. Moreover, the shapes of the distributions are quite independent of the target. The results are compared with modern optical-model predictions and with Intra-Nuclear Cascade (INC) calculations. Reasonable agreement between calculations and experimental data is obtained in the forward angles, but the comparison clearly indicates the need to modify the parameterization of the model at backward angles, where the agreement is rather poor.

PACS. 24.10.Ht Optical and diffraction models – 25.40.Ep Inelastic proton scattering – 28.90.+i Other topics in nuclear engineering and nuclear power studies

1 Introduction

With the present generation of intermediate-energy accelerators it is possible to study proton-induced nuclear reactions in an energy region where a number of potential large-scale applications are under development, or at least have been identified. These applications primarily fall into two categories: nuclear energy and waste [1], and nuclear medicine. For all these applications, an improved understanding of proton interactions is needed for calculations of proton transport and radiation effects. The nuclear data required for this purpose come almost entirely from nuclear scattering and reaction model calculations, which all depend heavily on the optical model, parameters of which are, in turn, determined by elastic scattering and total cross-section data [2].

The present work is part of the European project HINDAS (High and Intermediate energy Nuclear Data for Accelerator-driven Systems) [3], which has been designed to meet the demand for new nuclear data for feasibility assessments of accelerator-based transmutation techniques. Moreover, it provides a real testing ground for feasibility of different reaction models at this intermediate energy.

Proton-induced reaction data are also important for fundamental understanding of the nucleon-nucleus interaction. In particular, an incident projectile in the 50–200 MeV energy range can dislodge the deeply bound nucleons, and thus parts of the nucleus can be studied that are not accessible at lower energies, where the reactions are dominated by interactions with the valence nucleons. On the other hand, it should be possible to interpret the experimental results in terms of nucleon-nucleon collisions within a nucleus.

At 150–200 MeV proton energy, there have been very few proton-induced cross-section measurements, reported in the literature for ^{208}Pb, while there is none for ^{56}Fe and ^{238}U. An experiment [4] at the Indiana cyclotron facility was reported to have been performed at 165 MeV of proton energy with only two NaI(Tl) telescopes, in order to determine the absolute *p*-*p* cross-sections of ^{208}Pb at polar angles between 25°–150°. However, the results suffered a major uncertainty, to within 15%, due to the statistical uncertainty in the correction factor accounting for the dead-layer (in front of the NaI(Tl) crystal) contribution.

Here, we report on the measurement of multiplicity and differential cross-sections of protons from ^{56}Fe, ^{208}Pb, and ^{238}U targets at an incident proton energy of 190 MeV. This experiment was performed at the superconducting cyclotron facility, AGOR (Accélérateur Groningen ORsay) of the Kernfysisch Versneller Instituut (KVI). Singles proton spectra were obtained at a number of angles between 5°–30° and 91°–160°. The results are compared

[a] e-mail: mukherjee@kvi.nl

Table 1. Summary of targets used in the experiment.

Target	Thickness (mg/cm^2)	Isotopic Purity (%)
^{56}Fe	0.92	99.7
^{208}Pb	4.00	99.6
^{238}U	50.0	99.9

with modern optical-model predictions and with Intra-Nuclear Cascade (INC) calculations.

2 Experimental procedure

The experiment was conducted with several targets placed in the scattering chamber of the p-line associated with the SALAD (Small-Angle Large-Acceptance Detector) setup at KVI. Table 1 lists the targets with their thicknesses. The 190 MeV incident proton beam from the AGOR cyclotron lost a negligible amount of energy while traversing the target. The beam current varied between 0.1 and 0.2 nA and was limited by acceptable counting rates in the detectors. The beam halo, which may in principle be severe at forward angles, was monitored by a comparison of the count rate of particles scattered from an empty target frame with that of particles scattered from the target. Results reported here correspond to background rates of typically 0.5% to 1%, and were corrected for this effect wherever required.

Scattered protons were detected by two different detection systems, Plastic Ball [5] and SALAD [6], for two different angular domains, as is shown in fig. 1.

The spatial resolution and thus the number and dimensions of individual modules of Plastic Ball, are suitable to resolve the multiplicity distribution of particles from proton-induced reactions. Consisting of 340 ΔE-E particle-identifying detector modules, it covers a solid angle of up to nearly 50% of 4π, ranging in polar angle, $\theta = 91^\circ$ to 160°, with respect to the beam axis. Seven geometrical annular rings, each one defining a θ bin of approximately, 10°, hold the detector modules around the target position. The central spherical cavity of the ball has a radius of 25.4 cm, while the outer radius is 61.4 cm. Each ΔE counter is a 4 mm thick CaF_2(Eu) crystal with a characteristic decay time of 1 μs for the emission of the scintillation light. On the other hand, the light emission of the E counter, a 35.6 cm thick plastic scintillator, is approximately 100 times faster than that of the ΔE, so that 90% of the E signal is collected within 10 ns. The thickness of the ΔE counter allows a low-energy cut-off, around 25 MeV for protons, due to full energy deposition and complete stop in the ΔE counter, whereas the total length (36 cm) of each module ensures the identification of all the highly energetic protons produced in this experiment. These counters are optically coupled and read out by one photomultiplier with subsequent separation of the signals by pulse shape analysis.

The setup of SALAD, covering a solid angle of approximately 655 msr, detected the protons in the forward

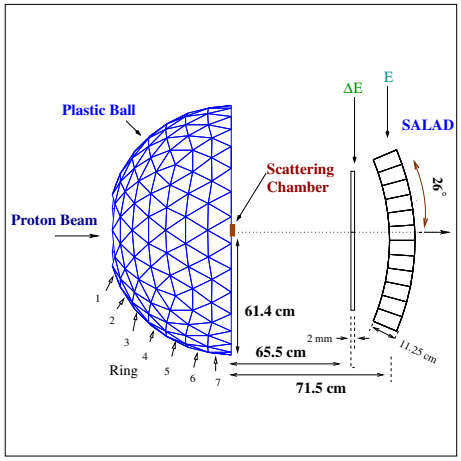

Fig. 1. A schematic top view of the experimental setup, showing both Plastic Ball (left) and SALAD (right). The beam pipe goes through the center of the entire detector setup.

angles, as is schematically shown in fig. 1. In this experiment, SALAD consisted of a ΔE plane of 24 thin scintillators, and an E plane of 24 thick scintillators. Protons are detected at polar angles between 5° to 30° with full azimuthal coverage below 26°. The counters in the ΔE plane are 2 mm thick plastic scintillators, which are assembled in two columns with each containing 12 horizontally placed strips, next to one another. Apart from the central four strips, each scintillator has a length of 630 mm and a width of 62 mm. The four central strips have a length of 450 mm each to allow space for the beam pipe. The 112.5 mm thick plastic scintillators in the E plane, ensuring a complete stop for 135 MeV protons, are aligned in two rows, each containing 12 of them. These strips are aligned in such a way that they form part of a cylinder with a radius of 71.5 cm around the target position. Each scintillator of E (ΔE) was read out via an 8-stage (12-stage) Phillips phototube, coupled via a light guide. The ΔE and E planes of SALAD were mounted such that they formed a grid among themselves, thereby acting effectively as a set of 144 ΔE-E telescopes in the forward angle. Since the energy loss for protons was considerably greater in the ΔE detector of SALAD than in the target, it is primarily the thickness of the ΔE detector that determines the low-energy cut-off, which comes around 20 MeV for protons. Similarly, protons with energies larger than 135 MeV (high-energy cut-off) punch through the E scintillator, and therefore, it becomes more difficult to identify them in SALAD. For the 190 MeV proton beam, it guarantees that all the elastically scattered protons will be detected but not identified on-line as they will not follow the conventional ΔE-E energy loss pattern. However, in the off-line analysis, elastically scattered protons are recognized by their typical energy deposition spectrum in the E detector. In this experiment, the individual scintillator rates of SALAD were around 10 kHz, while the Plastic Ball modules were operating at a rate of around 1 kHz. The SALAD CFD (Constant-Fraction Discriminator) signal was down-scaled and OR-ed with the

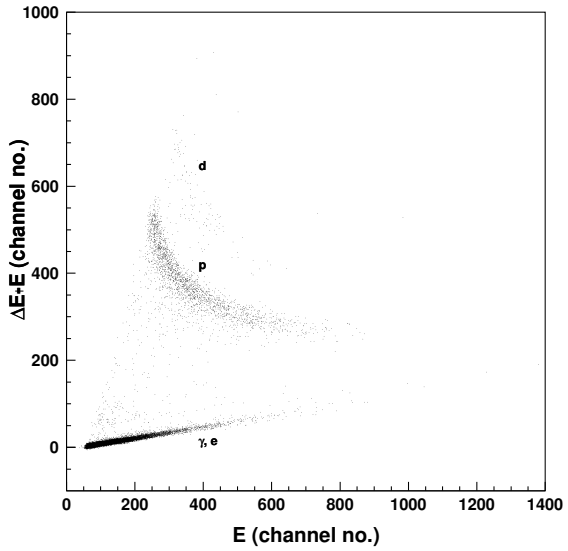

Fig. 2. A two-dimensional plot of $\Delta E + E$ *versus* E, revealing the excellence of the Plastic Ball to discriminate protons and other light charged particles (deuterons, in this case) from the mostly abundant γ's and leptons produced in this reaction.

down-scaled Plastic Ball signal, to generate the master trigger for data acquisition, with a rate around 250 Hz.

3 Data analysis

With an effective 24-hour beam time, a total of 4.1, 8.6, and 4.2 million events were recorded, respectively, for ^{56}Fe, ^{208}Pb, and ^{238}U targets. Subsequently in the off-line analysis, we exploited the energy and time information of each detector, in order to identify and isolate protons from γ's and other detected particles, like leptons, neutrons, deuterons or high-Z particles. In the analysis of Plastic Ball data, the events were selected with a prompt (self-trigger and/or coincidence) time window and a well-defined energy window for identifying protons. In fig. 2, a typical ΔE-E spectrum shows the quality of Plastic Ball for having an excellent identification and separation of protons from the background. It is the energy loss of the particles (lower branch in fig. 2), traveling with the speed of light (photons and leptons), that determines the cleanliness of separation from the relatively heavier protons and deuterons (respectively, middle and upper branches in fig. 2). The scattered events in the overlapping region between two neighboring branches, determine the major source of uncertainty in this singles measurement. However, as is evident from this spectrum, we found that the uncertainty of misidentifying a proton as a photon, or as a lepton is as low as nearly 2%, while that for a proton as a deuteron is less than a percent. This limit ensures the major source of systematic uncertainty in particle identification to be much below 5% for Plastic Ball. On the other hand, for the analysis of the SALAD data, we selected those events for which at least one ΔE and the

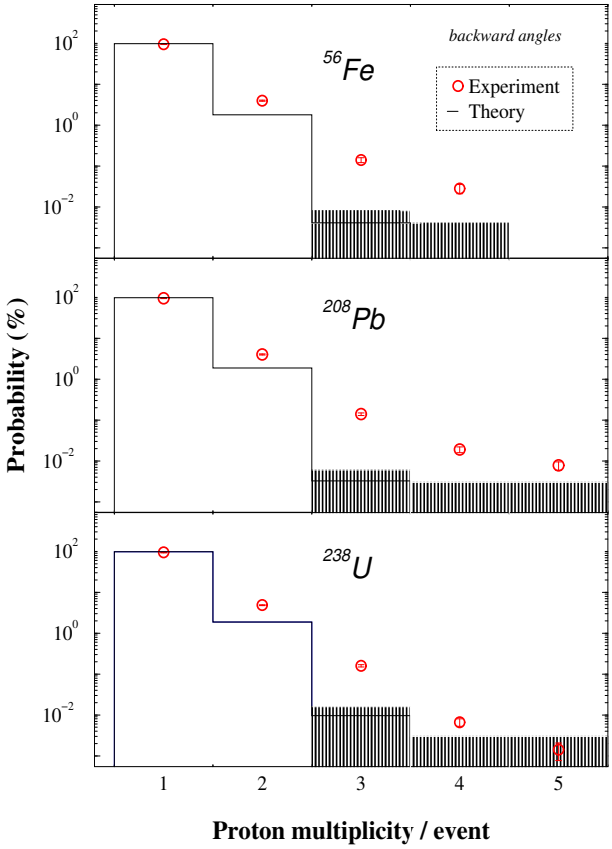

Fig. 3. Multiplicity distribution of protons observed in Plastic Ball ($95.1^\circ \leq \Theta_{\mathrm{c.m.}} \leq 156.1^\circ$), compared with the INC model predictions. The open circles represent the experimental data points, and the solid histograms the model calculations. The shaded area in the diagram represents the statistical upper limits inherent in the Monte Carlo code. See table 2 for details.

corresponding E scintillators have fired within the proper time window, thereby selecting protons which had either reached or punched through the E scintillator.

From the number of uncorrected proton events (N), the differential cross-section, $\frac{\mathrm{d}\sigma}{\mathrm{d}\Omega(\theta)}$, was derived within the accepted phase space covered by Plastic Ball and SALAD, by the formula

$$\frac{\mathrm{d}\sigma}{\mathrm{d}\Omega}(\theta) = 0.266 \cdot 10^{-3} \cdot \frac{A}{\mu} \cdot \frac{N}{(1-D) \cdot Q \cdot Y \cdot \Delta\Omega} \quad \left(\frac{\mathrm{mb}}{\mathrm{sr}}\right)$$

with
A = target mass (g/mol),
μ = target thickness (mg/cm^2),
D = dead time in fraction,
Q = integrated charge (nC),
Y = efficiency, and
$\Delta\Omega$ = solid angle (sr).

The total integrated charge, Q, was measured by a Faraday cup, while the dead time, D, of the acquisition system is experimentally determined using the scalar information of the triggers. The value of the total detection

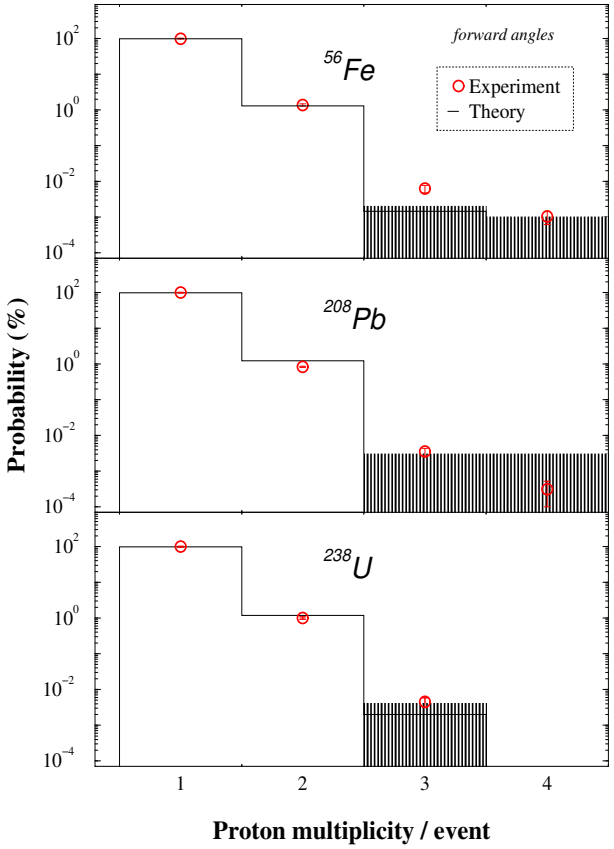

Fig. 4. Same as fig. 3, but for SALAD detector ($7.4^\circ \leq \Theta_{\rm c.m.} \leq 27.4^\circ$). See table 3 for details.

efficiency of Plastic Ball, about 100% for protons with energy more than 25 MeV, is obtained from the results of a simulation, using an event generator in combination with the detector simulation program GEANT3 [7]. A value of nearly 100% is estimated to be the efficiency of SALAD in detecting protons with energy exceeding 20 MeV. The uncertainties in these numbers enter into the estimation of the systematic error in the absolute values for the cross-sections. Due to the variation in the target thickness and uncertainties in the measurement of the Faraday cup, deviations will also arise in the estimation of luminosity. Taking into account all the uncertainties on the measured values, we obtain a systematic uncertainty of approximately 5% on average.

4 Results and comparison with model calculations

Here, the multiplicity distributions of protons per each event are compared with the theoretical predictions folded with the detector acceptance. As the Plastic Ball and SALAD, covering two different phase-space regions, have different detecting thresholds for protons and also because they acquired data in OR mode, we analysed the registered multiplicities in SALAD and Plastic Ball separately. Therefore, this distribution is disentangled in two different angular regions. In fig. 3, the multiplicity distribution of protons for Plastic Ball is shown, while fig. 4 shows the same for SALAD. The sum of the statistical and systematic uncertainties of the experimental data points, are much smaller than those shown in the figures. In the Intra-Nuclear Cascade (INC) calculations [8], the energy of protons is restricted to $E > 25$ MeV for Plastic Ball and $E > 20$ MeV for SALAD data. Tables 2 and 3 give the summaries of measured proton multiplicities with INC predictions for Plastic Ball and SALAD, respectively. In figs. 3 and 4, the measured data points (open circles)

Table 2. Comparison of measured proton multiplicity with INC predictions. A proton energy threshold of 25 MeV is taken into account for calculations with Plastic Ball angles. Here, the results for ^{56}Fe, ^{208}Pb, and ^{238}U targets, are shown. See text for details.

Target	Multiplicity of proton (/ event)	Observed probability [a] (%)	INC predictions (%)
^{56}Fe	1	95.89 ± 2.47	98.19 ± 0.63
	2	3.95 ± 0.12	1.80 ± 0.09
	3	0.140 ± 0.007	0.004 ± 0.004
	4	0.028 ± 0.002	< 0.004
^{208}Pb	1	96.79 ± 2.51	98.12 ± 0.57
	2	4.04 ± 0.12	1.88 ± 0.08
	3	0.140 ± 0.007	0.003 ± 0.003
	4	0.019 ± 0.002	< 0.003
	5	0.008 ± 0.001	< 0.003
^{238}U	1	94.98 ± 2.44	98.12 ± 0.56
	2	4.85 ± 0.14	1.87 ± 0.08
	3	0.160 ± 0.007	0.010 ± 0.006
	4	0.0070 ± 0.0008	< 0.003
	5	0.0014 ± 0.0003	< 0.003

([a]) These values are normalized with respect to the total number of events in Plastic Ball.

Table 3. Same as table 2 for forward angles (SALAD). See text for details.

Target	Multiplicity of proton (/ event)	Observed probability [a] (%)	INC predictions (%)
^{56}Fe	1	98.60 ± 2.53	98.70 ± 0.38
	2	1.38 ± 0.04	1.30 ± 0.04
	3	0.0060 ± 0.0007	0.001 ± 0.001
	4	0.0010 ± 0.0002	< 0.001
^{208}Pb	1	99.17 ± 2.53	98.77 ± 0.42
	2	0.83 ± 0.03	1.23 ± 0.05
	3	0.0035 ± 0.0004	< 0.003
	4	0.00030 ± 0.00009	< 0.003
^{238}U	1	98.99 ± 2.55	98.82 ± 0.43
	2	1.00 ± 0.03	1.18 ± 0.05
	3	0.0050 ± 0.0007	0.002 ± 0.002

([a]) These values are normalized with respect to the total number of events in SALAD.

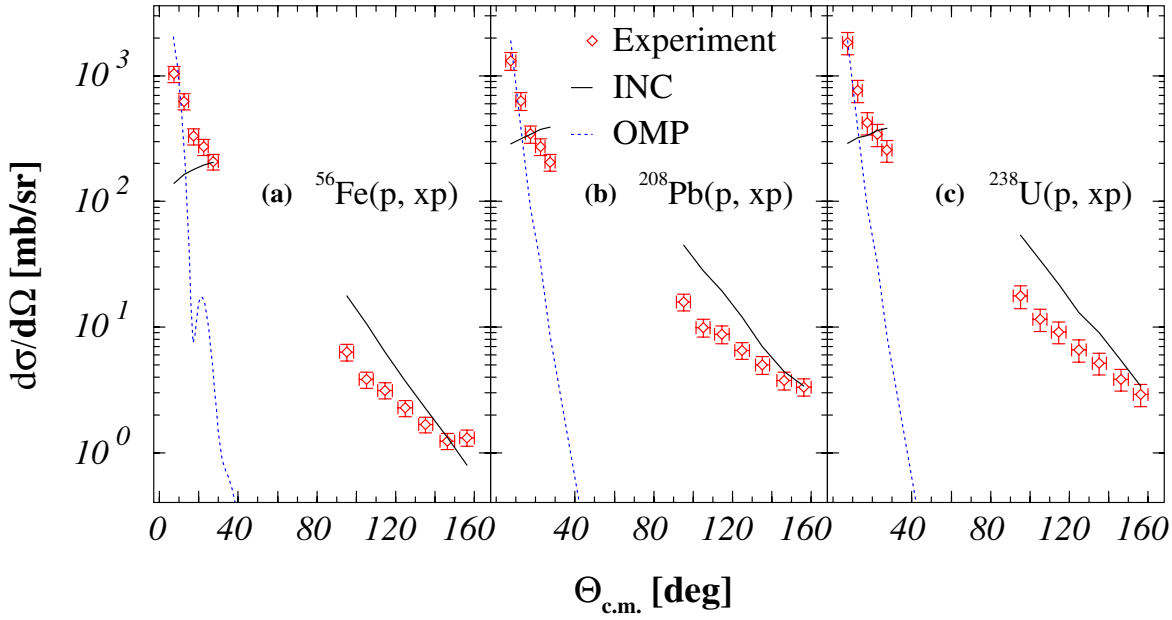

Fig. 5. Differential cross-sections of proton scattering from ^{56}Fe (panel a), ^{208}Pb (panel b), and ^{238}U (panel c) at 190 MeV incident proton energy. The open diamonds represent the experimental points, with the solid and dotted lines showing the INC and optical-model predictions, respectively. As there is no measurement in the angular range, 30°–91°, the INC calculation is not performed in this region. See tables 4-6 for details.

are compared with INC calculations (solid histograms). Here the experimental results and the INC calculations are normalized to 100% for multiplicity = 1. Overall, each measured spectrum is characterized by an exponential line (not shown in the Figures), starting with a huge contribution at multiplicity one, mainly attributed to the elastic contribution for forward angles, while completely non-elastic for backward angles. The maximum multiplicity, five protons per event that can be found at backward angles, in contrast to four at forward angles, is that of ^{208}Pb target. For ^{56}Fe, the maximum comes at four protons per event for both angular ranges, while for ^{238}U it is three and five, respectively, in the forward and backward angular ranges. This difference in maxima of multiplicity, for two different angular regions, is probably due to the difference in the phase-space coverage of the two detection systems. For high-multiplicity proton events, when one proton is detected in the Plastic Ball, there is a fair chance that a large portion of the rest of the protons in that event is also detected in it because of its large phase-space coverage. Whereas in case of SALAD, because of its relatively small phase-space coverage, the probability of one or more protons escaping detection is high, thereby, the high-multiplicity proton events would effectively appear as low-multiplicity events in SALAD. This, perhaps, explains why we fail to observe an event with five protons in SALAD in contrast to Plastic Ball.

To understand and interpret the observed multiplicity distributions in different angular ranges, we have carried out an extensive study with the INC model. In this model, the cascade process is seen as a time-ordered sequence of binary collisions occurring as in free space (except for Pauli blocking) between classical nucleons. This model has been proven to be quite successful in the description of the main features of proton-nucleus reactions in the GeV range [8]. Recently, it has been tested at lower energies (from 40 MeV to 250 MeV) as well, resulting in a good agreement in most of the cases [9]. This model has reproduced the measured values of multiplicity one very accurately for all targets in the angular coverages in both systems, although it should be pointed out that this model does not take into account the coherent elastic scattering. Moreover, the two-proton events are also reasonably well accounted for by the INC calculations. At forward angles (fig. 4), this calculation predicts rather well the proton multiplicity events for all three nuclei. But at backward angles (fig. 3), the INC goes on underestimating the yields of higher proton multiplicity events for all three nuclei. Overall, the INC underevaluates any event with more than two protons, with the situation being strikingly different for the case at backward angles, where it consistently underpredicts the events of higher (≥ 3) proton multiplicity by more than an order or so, with respect to the experimental data points.

As already outlined in the previous section, the angle-differentiated cross-sections are obtained by integrating over the azimuthal angle, ϕ. After correcting the data with the detector efficiencies and applying the normalization for covering the phase space, these values of cross-section are determined. These distributions of protons emitted from three targets, ^{56}Fe, ^{208}Pb, and ^{238}U, respectively, are presented in fig. 5. Tables 4-6 represent the summary of cross-section values for these targets. The data are compared with modern Optical-Model Potential (OMP) calculations using CHUCK3 [10], and with the INC calculations to account for all possible reaction channels contributions. As

Table 4. Values of measured cross-sections of the ^{56}Fe(p, xp) reaction at 190 MeV, compared with the Optical-Model Potential (OMP) and INC predictions. Proton energy thresholds of 20 and 25 MeV are taken into account for calculations, respectively, for SALAD and Plastic Ball angles. See text for details.

$\Theta_{\mathrm{c.m.}}$ [a], [b] (degree)	$\frac{\mathrm{d}\sigma}{\mathrm{d}\Omega}\big\vert_{\mathrm{Exp.}}$ (mb/sr)	$\frac{\mathrm{d}\sigma}{\mathrm{d}\Omega}\big\vert_{\mathrm{OMP}}$ (mb/sr)	$\frac{\mathrm{d}\sigma}{\mathrm{d}\Omega}\big\vert_{\mathrm{INC}}$ (mb/sr)
7.4	1035.9 ± 25.9	1615	139
12.4	624.8 ± 15.6	351.5	163
17.4	330.1 ± 8.3	7.6	179
22.4	272.4 ± 6.8	17.2	195
27.4	207.0 ± 5.2	4.9	204
95.1	6.3 ± 0.2	6.9×10^{-6}	17.7
105.0	3.8 ± 0.1	4.9×10^{-6}	10.6
114.6	3.10 ± 0.08	8.3×10^{-7}	6.3
124.8	2.20 ± 0.06	2.0×10^{-7}	3.7
135.2	1.60 ± 0.04	2.1×10^{-7}	2.3
146.2	1.20 ± 0.03	1.3×10^{-6}	1.3
156.1	1.30 ± 0.03	1.9×10^{-7}	0.8

([a]) Forward (SALAD) angles 7.4°–27.4°.
([b]) Backward (Plastic Ball) angles 95.1°–156.1°.

Table 5. Same as table 4 for the ^{208}Pb(p, xp) reaction.

$\Theta_{\mathrm{c.m.}}$ (degree)	$\frac{\mathrm{d}\sigma}{\mathrm{d}\Omega}\big\vert_{\mathrm{Exp.}}$ (mb/sr)	$\frac{\mathrm{d}\sigma}{\mathrm{d}\Omega}\big\vert_{\mathrm{OMP}}$ (mb/sr)	$\frac{\mathrm{d}\sigma}{\mathrm{d}\Omega}\big\vert_{\mathrm{INC}}$ (mb/sr)
7.4	1315.0 ± 32.9	1894	288
12.4	629.0 ± 15.7	382.6	314
17.4	344.0 ± 8.6	89.1	342
22.4	272.0 ± 6.8	31.9	375
27.4	205.0 ± 5.1	8.5	390
95.1	15.7 ± 0.4	7.4×10^{-6}	45
105.0	9.8 ± 0.2	1.8×10^{-6}	29
114.6	8.7 ± 0.2	6.4×10^{-7}	19
124.8	6.5 ± 0.2	1.7×10^{-7}	12
135.2	5.0 ± 0.1	9.6×10^{-8}	7
146.2	3.7 ± 0.1	7.9×10^{-8}	4.4
156.1	3.3 ± 0.1	2.9×10^{-8}	3.4

Table 6. Same as table 4 for the ^{238}U(p, xp) reaction.

$\Theta_{\mathrm{c.m.}}$ (degree)	$\frac{\mathrm{d}\sigma}{\mathrm{d}\Omega}\big\vert_{\mathrm{Exp.}}$ (mb/sr)	$\frac{\mathrm{d}\sigma}{\mathrm{d}\Omega}\big\vert_{\mathrm{OMP}}$ (mb/sr)	$\frac{\mathrm{d}\sigma}{\mathrm{d}\Omega}\big\vert_{\mathrm{INC}}$ (mb/sr)
7.4	1836.4 ± 45.9	1894	290
12.4	764.9 ± 19.1	382.6	320
17.4	422.8 ± 10.6	89.1	335
22.4	340.4 ± 8.5	31.9	365
27.4	255.7 ± 6.4	8.5	380
95.1	17.6 ± 0.4	7.4×10^{-6}	54
105.0	11.5 ± 0.3	1.8×10^{-6}	34
114.6	9.1 ± 0.2	6.4×10^{-7}	22
124.8	6.6 ± 0.2	1.7×10^{-7}	13
135.2	5.2 ± 0.1	9.6×10^{-8}	09
146.2	3.8 ± 0.1	7.9×10^{-8}	5.4
156.1	2.9 ± 0.1	2.9×10^{-8}	3.4

the theoretical curves deduced from OMP calculations, unlike INC, are not folded with the experimental angular resolution, comparisons are rather qualitative. The quality of the present normalization is rather fair as can be judged by comparing to the differential elastic cross-section calculated at very small angles for these systems. The data points (open diamonds) are compared with model predictions in fig. 5, where the solid and dotted lines represent the INC and OMP calculations, respectively. By tuning the energy threshold for proton detection, within ±5 MeV, in INC calculation, leads to a relative fluctuation of approximately ±5% within the calculated cross-section values.

We have performed a series of OMP calculations with CHUCK3, employing a global nucleon-nucleus Optical-Model Potential for ^{56}Fe, ^{208}Pb, and ^{238}U [11]. This OMP is valid for incident nucleon energies between 1 keV and 200 MeV and masses from 24 to 209. It is based on a smooth functional form for the energy dependence of the potential depths, and on physically constrained geometry parameters. An extensive collection of experimental data sets for different types of observables was used to determine the parameters of the OMP.

When comparing these predictions with the data, a few striking features appear evident. First, optical-model calculations for elastic scattering are in reasonably good agreement at small angles, as they should with all the data sets. It should be pointed out that none of the predictions of the optical model uses parameters adjusted to the present experiment. In fact, they were all made available before the data were obtained. Even the absolute scale seems to be under remarkably good control. Particularly, for ^{208}Pb and ^{238}U data sets, the first two data points at small angles are in good agreement with the OMP calculations, thereby increasing the confidence of good normalization of the data. However, in ^{56}Fe a large discrepancy is observed at the smallest angle, maybe, arising from the global OMP, which has been used for this nucleus. At relatively larger angles, the contribution from the elastic cross-section drops sharply, and therefore, becomes completely insignificant for Plastic Ball data at backward angles. In this region and further backward non-elastic channels start dominating over the elastic one. The quality of OMP predictions is quite equivalent for Fe and Pb, while this is even better for U which is actually performed with an extrapolation of the optical-model parameters.

Second, the INC model calculations are, more or less, in good agreement with the experiment. Particularly, for ^{56}Fe data the INC calculation accounts well for the backward-angle cross-section values. However, there exist some overestimations, at most by a factor of two to three, for some experimental points at 91°–120°. But at the most backward angles, the calculation smoothly converges with the experimental values. The most noticeable feature of these calculations is that for forward angles they are reasonably in good agreement with the data, since the elastic-scattering contribution dominates in this region. The disagreement between INC model and the experiment for the backward angles is not expected as is

reported in ref. [9]. For the heavier targets, like ^{238}U, its general pattern in our calculations indicates that proton emission is much too forward peaked, which translates into an overestimation of the differential-cross-section values. This discrepancy should not be overemphasized because of the fact that the INC model, which assumes mean-field properties of nuclei to be dominant, can have problems in describing deformed nuclei. This model assumes spherical nuclei. Although the nuclei considered here are known to be spherical in nature, except ^{238}U, a co-existence of deformation degrees of freedom in spherical nuclei might result in deviations from the results predicted by INC. The same remark should probably be made for the events where the multiplicity is equal to four or more. These events are rare and the results obtained with the INC model are possibly underestimated (the number of runs performed for each INC calcuation is 500000).

5 Conclusions

In short, a study of proton-induced reactions is carried out at KVI with the Plastic Ball + SALAD configuration, measuring the multiplicity and differential cross-sections of protons over a broad angular region. The present investigation has resulted in a data set for three nuclei, namely, ^{56}Fe, ^{208}Pb, and ^{238}U at 190 MeV of proton energy, for the first time in this energy range. The overall agreement with model predictions, both OMP and INC, is reasonable. However, a detailed account of all aspects of INC calculations shows that, particularly at backward angles, it disagrees with the experiment by at most a factor of two to three, which triggers a need for improvement of the INC model, at least to reproduce the smooth angular-distribution pattern over the range investigated. The disagreement with the experiment and the INC model for the higher proton multiplicity events at backward angles, might imply that the statistical evaporation part of the decay process is not properly accounted for in the model. This could perhaps shed light on the reasons for the higher-multiplicity pattern observed in this experiment.

The authors wish to thank the operating crew of the cyclotron facility at KVI for skillful assistance. We also gratefully acknowledge the helpful discussions with Prof. J. Cugnon, Université de Liège (Belgium), and with Dr. A.J. Koning of NRG, Petten (The Netherlands). We thank GSI, Darmstadt (Germany) for the loan of the Plastic Ball. This work was supported by the HINDAS project of the EU framework program under Contract No. FIKW-CT-2000-00031.

References

1. C.D. Bowman, Annu. Rev. Nucl. Part. Sci. **48**, 505 (1998).
2. J. Klug *et al.*, Phys. Rev. C **67**, 031601(R) (2003).
3. A. Koning *et al.*, J. Nucl. Sci. Technol. **2**, 1161 (2002).
4. R.E. Segel *et al.*, Phys. Rev. C **26**, 2424 (1982).
5. A. Baden *et al.*, Nucl. Instrum. Methods **203**, 189 (1982).
6. N. Kalantar-Nayestanaki *et al.*, Nucl. Instrum. Methods A **444**, 591 (2000).
7. R. Brun *et al.*, GEANT3 Users Guide, Data Handling Division DD/EE/84-1, CERN (1986).
8. J. Cugnon *et al.*, Nucl. Phys. A **620**, 475 (1997).
9. J. Cugnon, P. Henrotte, Eur. Phys. J. A **16**, 393 (2003).
10. P.D. Kunz, University of Colorado, 1983, unpublished; B. Mukherjee *et al.*, Internal Report (KVI) (2003).
11. A.J. Koning, J.P. Delaroche, Nucl. Phys. A **713**, 231 (2003).